

Fatigue strength assessment of welded joints in the marine environment – A case study on the applications of local stress and fracture mechanics methods for analyzing non-load-carrying fillet-welded joints

Antti Ahola¹, Timo Björk

Summary Welding is a commonly applied joining method in many applications in arctic and marine conditions, e.g., in ship and offshore structures, and energy production equipment. Such applications are usually subjected to fluctuating load conditions, and during a decades-long service, they may experience millions of load cycles. Consequently, fatigue strength design and acceptable flaw sizes in the welded details of these structures are among the most important design criteria. Multiple fatigue strength assessment approaches exist for assessing the fatigue strength of a welded detail. The present study introduces a numerical and analytical fatigue strength assessment, conducted on a non-load-carrying X-joint, which is a representative joint type used in many steel constructions. Fatigue analyses are carried out following the DNVGL-RP-C203 and BS7910:2013 fatigue design guidelines for offshore steel structures. The stress intensity factors (SIFs) for linear elastic fracture mechanics (LEFM) analyses were obtained using three different methods: the weight function approach, the analytical equations provided in the IIW Recommendations, and by conducting numerical crack propagation analysis using the Franc2D software. All three methods had a good agreement particularly for short crack depths, indicating the applicability of the analytical approaches for the fatigue analyses. The results showed that the consideration of degree of bending at the welded detail is crucial due to the distinguishing notch stress factors of membrane and bending loading, and different stress distributions in the through-thickness direction. In addition, it was found that the LEFM-based fatigue life assessments are significantly more conservative than the life predictions obtained using the structural hot-spot and effective notch stress approaches.

Keywords: welded joint, fatigue, stress intensity factor, linearly elastic fracture mechanics, effective notch stress

Received: 16 November 2022. Accepted: 1 February 2023. Published online: 2 May 2023.

¹Corresponding author: antti.ahola@lut.fi

Introduction

In arctic conditions, structures are exposed to low ambient temperatures, which does not usually have a major effect – or at least has only a minor beneficial effect [1,2] – on the fatigue performance of welded steel structures, unless the temperature goes beneath the transition temperature. However, many applications in such arctic areas also incorporate the marine environment. Structures in marine environment are typically subjected to different fluctuating loads, such as wave and wind loads and, in arctic applications, ice loads. The cyclic behavior in loads causes fluctuating stresses in the weldments of such structures, predisposing the welded components to fatigue failures. On the other hand, the increasing need to decrease material usage has led to the optimization of structures and consequently, an increase in stress range levels. Hence, fatigue design and analysis should be carried out for a finite fatigue life, instead of targeting the infinite life of welded components.

Existing design codes [3–6] provide multiple approaches to assess the fatigue strength of welded details, including stress-based approaches, such as the structural hot-spot (HS) stress method and effective notch stress (ENS) concept, and fracture mechanics-based analyses that, in fatigue assessments, are typically conducted using linear elastic fracture mechanics (LEFM). In the present paper, fatigue analyses are carried out for a non-load-carrying X-joint, which is a representative joint type existing in many steel constructions. The fatigue strength is assessed using the HS and ENS concepts, and the LEFM analyses are conducted on the basis of the stress intensity factors (SIFs) obtained using the analytical equations, weight function (WF) approach, and numerical crack propagation analysis. Furthermore, the influence of the degree of bending (DOB, equal to bending stress divided by total stress) on the fatigue strength assessment is also evaluated. Structures in a marine environment with and without cathodic protection are considered within this study.

Materials and methods

Geometry and materials of the studied joint

This paper investigates a non-load-carrying (NLC) cruciform joint made of mild steel material, which is representative of many applications in arctic conditions. The dimensions of the joint (Fig 1a) are taken from an industrial case in which the joint is subjected to a load corresponding to an equivalent HS stress of $\Delta\sigma_{hs,eq} = 29.2$ MPa ($m = 3$), as shown in Fig. 1b. Considering the fabrication process, K-butt welds (Fig. 1) usually result in external fillet welds. In this study, a leg length of $z = 8$ mm was assumed with the flank angle of $\theta = 50^\circ$ considering the studied K-butt joint configuration. Furthermore, the plate misalignment effects [7] on the stress concentrations at the weld toe were neglected.

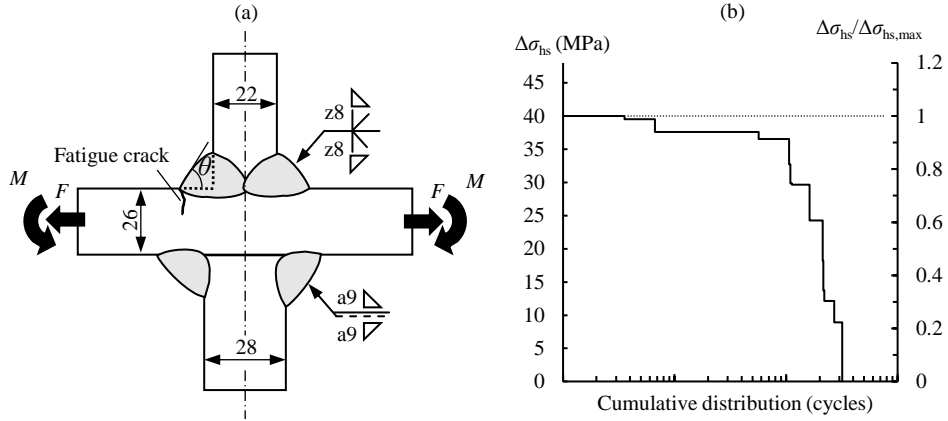


Figure 1. (a) Dimensions of the non-load carrying X-joint under investigation and (b) the obtained service load histogram.

Load conditions

The DOB for the case under investigation was not specified (structural stress obtained through the surface extrapolation method), two alternative load cases were considered in the analyses: axial membrane loading with a uniform stress distribution over the base plate ($t = 26$ mm) and pure out-of-plane bending loading (Fig. 1a) to observe the differences in the results for two different load cases. In the case of the stress-based approach, the fatigue strengths for the combined membrane and bending stress (DOB = 0–1.0) load cases can be derived from the DOB = 0 and DOB = 1 load cases by the superposition principle, but in the case of the LEFM-based fatigue analysis, the fatigue strength should be assessed using the predetermined DOB value. The fatigue analyses are carried out using 1 MPa unit loads but the fatigue life estimations are reflective of the given service load histogram (Fig. 1b).

Applied fatigue analysis methods

Linear elastic fracture mechanics

LEFM analyses were carried out using three different methods, namely analytical equations, the weight function (WF) approach and numerical crack propagation analysis, to compare the applicability of these methods to assess the SIFs and crack propagation rate and to thus predict the fatigue strength of the detail. The IIW Recommendations [4] provide the analytical formulae for the stress magnification factors M_k of X-joints, following earlier works undertaken by Hobbacher [8,9], whereby the SIF can be estimated as follows:

$$K = M_k(a)Y\sigma\sqrt{\pi a}, \quad (1)$$

where a is the crack size, σ is the normal stress acting at the base plate perpendicular to the crack (gross cross-section), and Y is the crack shape function. The M_k formulae are, however, available only for the membrane stress loading case. The WF approach is

applicable for both membrane and bending stress load cases, and the SIF can be calculated using the following formula:

$$K = \int_{x=0}^{x=a} \sigma(x)M(x,a)dx, \quad (2)$$

where $\sigma(x)$ is the normal stress distribution in the through-thickness direction (from the weld toe) and $M(x,a)$ is the weight function. The standard case is limited to crack shape aspect ratios of $a/c = 0.2$ – 1.0 , and in this case, $a/c = 0.2$ (low depth to width ratio) was conservatively assumed. The $\sigma(x)$ distributions for the WF analyses were obtained numerically using a 2D plane strain element model. The obtained distribution for a 1 MPa membrane and bending unit loads are shown in Fig. 2.

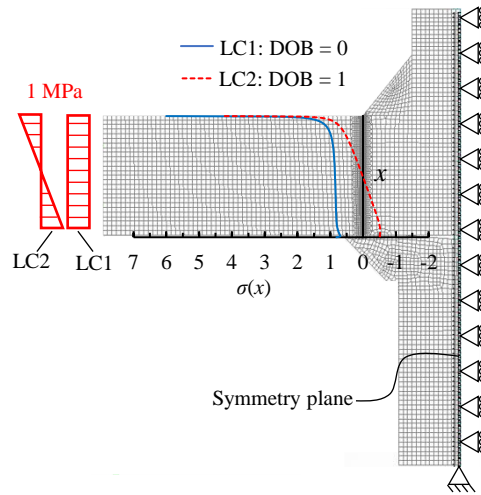


Figure 2. Stress distributions $\sigma(x)$ at the weld toe to the through-thickness direction.

Franc2D [10] crack propagation analyses were carried out to numerically obtain the SIF ranges for the given joint and load configurations. The FE model with the initial crack, and the crack paths obtained using maximum tangential stress criterion are shown in Fig. 3. The SIF ranges were obtained using a J-integral approach embedded in the Franc2D program. The resulting SIF values for all applied methods are presented in Fig. 4.

The fatigue life estimation was derived using Paris' crack propagation law, as follows:

$$\frac{da}{dN} = C\Delta K(a)^m \Rightarrow N_f = \int_{a_i}^{a_f} \frac{da}{C\Delta K(a)^m}, \quad (3)$$

where C is the crack propagation coefficient, m is the slope parameter of Paris' law, $\Delta K(a)$ is the SIF range as a function of crack depth, a_i and a_f are the initial and final crack depths, respectively, and N_f is the fatigue life. In the life assessments, an initial crack size of $a_i = 0.15$ mm was assumed as per the IIW Recommendations [4]. The

applied C and m values are presented in Table 1. In the shell structure under investigation, a high applied stress ratio R can be assumed due to the high tensile residual stresses present in large-scale structures. The recommended values are applicable for steels (excluding austenitic and duplex stainless steels) with yield strength up to 600 MPa.

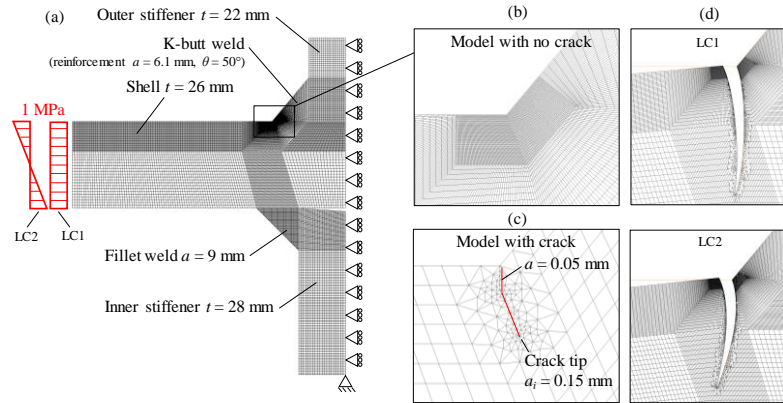


Figure 3. Franc2D model with (a) load and boundary conditions, (b) detailed mesh at the weld toe, and (c) inserted crack ($a = 0.05$ mm) which was subsequently propagated to $a_i = 0.15$ mm initial crack size, and (d) estimated failure paths.

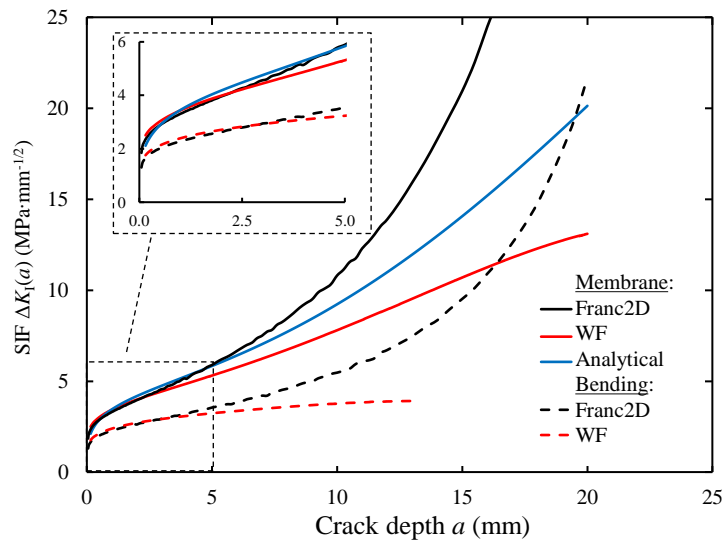


Figure 4. SIF values for 1 MPa membrane and bending stress unit loads.

Table 1. Crack propagation coefficients in a marine environment after BS7910 [11] for an applied stress ratio of $R \geq 0.5$ (Stage A, mean + 2 standard deviation), ΔK in unit $\text{MPa}\cdot\text{mm}^{-1/2}$.

Condition	C	m
Free corrosion	$1.72 \cdot 10^{-13}$	3.42
Cathodic protection (-1100 mV Ag/AgCl)	$2.10 \cdot 10^{-17}$	5.10

Structural hot-spot stress method

Structural stress comprises the membrane and bending stress components that are used in fatigue strength assessment [12]. Although the effect of DOB on the fatigue performance has been recognized, the stress components are not considered in the structural HS stress approach. While crack propagation has a dominating role in terms of the total fatigue life, i.e., considering both crack initiation and propagation, DNV-GL [3] allows a 40% reduction in the bending stress component. In addition, British Standards [6] provides an improvement factor for the fatigue strength capacity of joints with an increasing share of bending stress. However, neither the IIW Recommendations [4] nor Eurocode 3 [5] include a reduction for bending stress or an improvement factor for fatigue strength for joints subjected to bending. Engineers usually refrain from making unconservative fatigue strength predictions and, thus, the beneficial effect of DOB on the fatigue strength capacity is neglected. Consequently, $FAT = 100$ MPa for cathodic protection and $FAT = 62.4$ MPa for free corrosion are used in this study.

Effective notch stress concept

The ENS concept was employed applying the reference radius of $r_{ref} = 1.00$ mm [13] on the basis of effective stress concept with the fatigue notch factor of $K_f = K_t(r_{ref})$ assuming sharp transition from the base metal to the weld reinforcement ($r_{true} = 0$). As shown in [14,15], axial membrane and bending stresses induce different SCFs and result in different fatigue strength capacities and, consequently, the FE analyses were carried out using both load conditions. Fig. 5 shows the FE model used in the analyses. As a reference curve for the fatigue strength predictions, $FAT = 225$ MPa and $FAT = 156$ MPa with the recommended slope parameter of $m = 3$ were used following the DNV-GL guideline [3] for cathodic protection and free corrosion, respectively.

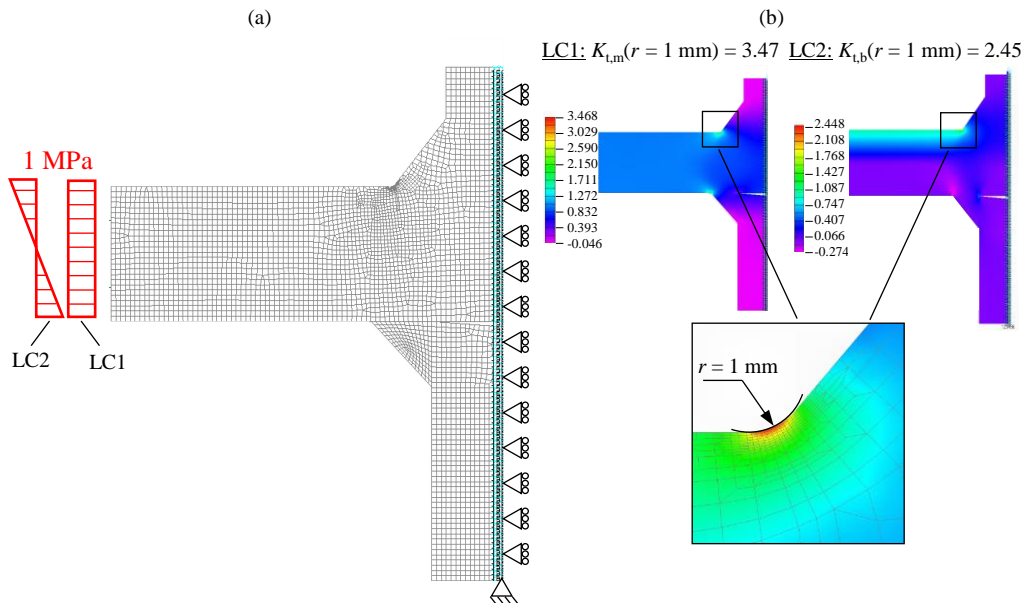


Figure 5. (a) ENS model with load and boundary conditions, and (b) the SCF for the membrane and bending stress components. The mesh size at the weld toe was 0.025 mm ($r/40$) in the radial direction, and 0.05 mm ($r/20$) in the tangential direction.

Results

The results of the fatigue analyses are summarized in Fig. 6 which presents the fatigue life predictions corresponding to the equivalent loading, i.e., $\Delta\sigma_{hs,eq} = 29.2$ MPa ($m = 3$) as per the load histogram shown in Fig. 1b. The LEFM analyses had a good correspondence in terms of fatigue life estimation but, however, they estimated conservative fatigue life estimations in comparison to the HS stress and ENS approaches.

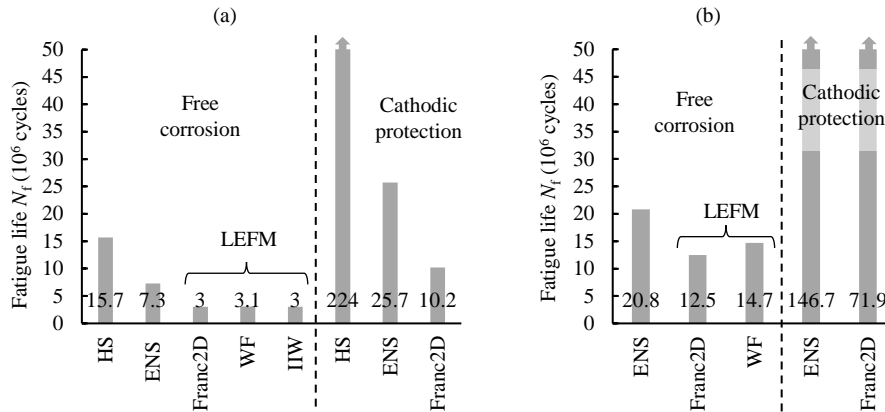


Figure 6. Results of the fatigue analyses for (a) DOB = 0 and (b) DOB = 1. The LEFM analysis conducted using the analytical equations (a membrane load case) is denoted with IIW.

In arctic and marine conditions, the influencing load cycles are usually fully random in service, i.e., the sequence of different load cycles shown in Fig. 1b is arbitrary. Consequently, a consideration of the threshold limit of the SIF causing crack propagation (proposed as $\Delta K_{th} = 63$ MPa \cdot mm $^{-1/2}$), the equivalent stress ranges depends on the crack depth since all load cycles are not effective at the early stage of crack propagation. Fig. 7 demonstrates the SIF ranges for different stress ranges and the resulting equivalent loading as a function of crack length a . In the case of axial loading and the given load histogram, no major effect on the equivalent loading was found but in the case of bending, due to the lower SIF values, the threshold limit was exceeded only with the 40.2 MPa and 39.7 MPa loads when $a_i = 0.15$ mm.

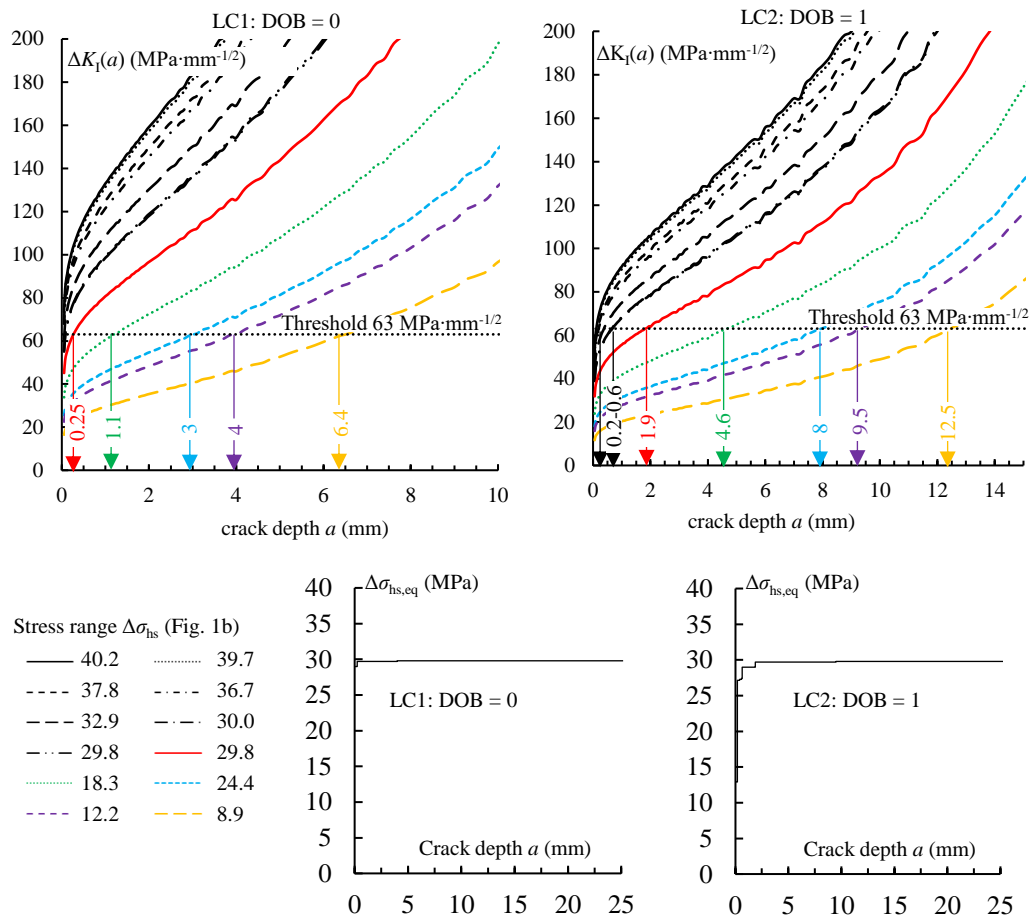


Figure 7. Effect of consideration of threshold limit on the equivalent HS stress range for membrane and bending stress load cases using the given load histogram.

Discussion and conclusions

In the present paper, fatigue analyses were conducted on a non-load-carrying X-joint, which is a common joint type in many steel structures. A corrosive marine environment was assumed, and the fatigue analyses were carried out assuming two conditions, namely a structural detail either with or without cathodic protection to investigate the influence on the fatigue strength capacity. A HS stress range equal to $\Delta\sigma_{hs,eq} = 30.4 \text{ MPa}$ ($m = 3$) and stress range representative of such welded details in arctic structures was taken as a basis for the fatigue assessments. Three different approaches, namely the structural HS stress and ENS concepts and LCFM were applied in the fatigue analyses. In addition, the effect of DOB was investigated by conducting the analyses assuming pure membrane (DOB = 0) and bending (DOB = 1) loads.

In the case of axial loading, the analytical equations [4], the WF approach and the numerically obtained SIF ranges had very good agreement, particularly for small crack sizes. Due to the pronounced effect of early crack propagation on the total fatigue life, all applied methods resulted in similar fatigue strength estimations, see Fig. 6. If the critical flaw sizes and SIFs, in terms of a brittle failure, are estimated, then the use of analytical equations and the WF approach may result in unconservative assumptions,

see Fig. 4. The analytical equations were not available for the $DOB = 1$ loading and, consequently, only the WF approach and numerical analyses were employed, resulting in similar fatigue strength estimations.

When comparing the fatigue strength assessments acquired using the LEFM and stress-based approaches, it can be noted that the LEFM resulted in much lower fatigue strength estimations than the stress-based approaches. In the case of LEFM, an initial crack size of $a_i = 0.15$ mm was assumed following the IIW Recommendations [4]. Thus, it can be concluded that smaller allowable initial crack sizes, or no initial cracks, should be assumed if the stress-based approaches are used. Particularly, for the ENS approach, no initial cracks should be present, and a certain period of crack initiation should thus be assumed. From the fabrication point of view, this puts pressure on achieving high welding quality, as well as managing quality assurance at least in fatigue-critical details. It is also worth noting that the crack propagation analyses were carried out assuming conservatively load-controlled behavior. In details such as those under investigation, the structure may also have displacement-controlled behavior which decreases the crack propagation rate. Based on the fatigue analyses and comparisons, the following conclusions can be summarized:

- In the investigated 2D NLC cruciform joint type, the WF approach and analytical equations by the IIW provide a good accuracy for the SIF values at the small crack depths up to $a/t = 0.2$, compared to the SIFs numerically obtained by the FE analyses. At the large cracks, the WF and analytical approaches are not necessarily sufficient to estimate SIF values. However, in fatigue assessments and life predictions, the crack growth behavior at the short crack regime has a dominating role and the WF approach and analytical equations can be thus recommended for such purposes.
- A consideration of DOB in the fatigue analyses is important; a higher fatigue strength was obtained for joints subjected to bending in the investigated joint type.
- Fatigue strength assessments assuming cathodic protection result in an approximately three times higher fatigue life compared to the air condition.
- A use of stress-based approaches resulted in higher fatigue strength predictions with respect to the LEFM analyses with an initial crack size of $a_i = 0.15$ mm and, hence, careful consideration of achievable welding quality should be noted in the fatigue design of such details.

References

- [1] R. Bridges, S. Zhang, V. Shaposhnikov. Experimental investigation on the effect of low temperatures on the fatigue strength of welded steel joints. *Ships and Offshore Structures*, 7:311–319, 2012. <https://doi.org/10.1080/17445302.2011.563550>
- [2] M. Braun, R. Scheffer, W. Fricke, S. Ehlers. Fatigue strength of fillet-welded joints at subzero temperatures. *Fatigue & Fracture of Engineering Materials & Structures*, 43:403–416, 2020. <https://doi.org/10.1111/ffe.13163>
- [3] DNVGL-RP-C203. *Fatigue Design of Offshore Steel Structures*, 2016.

- [4] A. Hobbacher. *Recommendations for Fatigue Design of Welded Joints and Components*, 2nd edition, Springer International Publishing, Cham, 2016.
- [5] EN 1993-1-9. *Eurocode 3: Design of steel structures – Part 1-9: Fatigue*, 2005.
- [6] BS7608:2014+A1:2015. *Guide to Fatigue Design and Assessment of Steel Products*, 2015.
- [7] A. Ahola, T. Björk. Fatigue strength of misaligned non-load-carrying cruciform joints made of ultra-high-strength steel. *Journal of Constructional Steel Research*, 175:106334, 2020. <https://doi.org/10.1016/j.jcsr.2020.106334>
- [8] A. Hobbacher. Stress intensity factors for welded joints. *Engineering Fracture Mechanics*, 46:173–182, 1993.
- [9] A. Hobbacher. Corrigendum, *Engineering Fracture Mechanics*, 49:323, 1994.
- [10] Cornell Fracture Group. Software. 16.11.2022. <http://cfg.cornell.edu/software/>
- [11] BS7910:2013+A1:2015. *Guide to methods for assessing the acceptability of flaws in metallic structures*, 2015.
- [12] E. Niemi, W. Fricke, S.J. Maddox. *Fatigue Analysis of Welded Components: Designer’s Guide to the Structural Hot-Spot Stress Approach*, 2nd edition, Springer Nature, Singapore, 2018. <https://doi.org/10.1533/9781845696665>
- [13] W. Fricke. *IIW Recommendations for the Fatigue Assessment of Welded Structures by Notch Stress Analysis*. IIW-2006-09, Woodhead Publishing, 2012.
- [14] A. Ahola, T. Nykänen, T. Björk. Effect of loading type on the fatigue strength of asymmetric and symmetric transverse non-load carrying attachments. *Fatigue & Fracture of Engineering Materials & Structures*, 40:670–682, 2017. <https://doi.org/10.1111/ffe.12531>
- [15] A. Ahola, T. Björk. Bending effects on the fatigue strength of non-load-carrying transverse attachment joints made of ultra-high-strength steel. In: A. Zingoni (Ed.), *Proceedings of 8th International Conference Structural Engineering, Mechanics and Computation (SEMC 2022)*, September 5–7, 2022, Cape Town, South Africa, 2022: pp. 1130–1135. <https://doi.org/10.1201/9781003348443-184>

Antti Ahola, Timo Björk
 Laboratory of Steel Structures, LUT University
 Yliopistonkatu 34, 53850, Lappeenranta, Finland
 antti.ahola@lut.fi, timo.bjork@lut.fi